Beam Tests of Quartz Radiators for Precision Timing Profile Monitor

Lee Teng Summer Research Project
Mentor: Eric Prebys
August 12, 2016

Rachel Margraf

Accelerator Division
Fermi National Laboratory, Batavia, IL 60510

1 Abstract:

Mu2e will look for neutrino-less conversion of a muon to an electron by capturing a muon around an aluminum nucleus. Expected backgrounds occur shortly after proton arrival, and can be eliminated utilizing a pulsed proton beam with tight constraints on out-of-time protons. The ratio of out-of-time protons to in-time protons is referred to as the extinction of the beam. The final Mu2e experiment requires an extinction of 10^{-10}, which is achieved using a system of resonant dipoles and collimators, but relies on an extinction of 10^{-5} during the beam production. The Precision Time Profile Monitor (PTPM) will measure the time structure both in the Fermilab Recycler and in the Mu2e beam, which will be extracted from the Delivery Ring, by building a statistical profile of protons at the 10^{-5} level. Here we conduct a beam test of Quartz Cherenkov Radiators for this PTPM to examine their response to 120GeV relativistic protons. The Quartz Radiators had about 99% detection efficiency with a time resolution of about 1ns. We estimate after pulsing to produce false signals at a rate less than 2 x 10^{-18}.

2 Introduction:

Mu2e will search for Charged Lepton Flavor Violation (CLFV) in the form of a neutrino-less conversion of a muon to an electron plus a photon or other particle ($\mu \rightarrow e + \gamma$). CLFV is incorporated into many beyond the standard model theories, but has yet to be observed in the laboratory. Previous experiments, most recently the SINDRUM II experiment in Switzerland, excluded this decay with a branching ratio of $R_{\mu e} \leq 7 \times 10^{-13}$. Mu2e is designed to detect events as rare as $R_{\mu e} \approx 10^{-17}$.

$$R_{\mu e} = \frac{\mu^- + A(Z,N) \rightarrow e^- + A(Z,N)}{\mu^- + A(Z,N) \rightarrow \nu_\mu + A(Z-1,N)}$$

Mu2e produces muons by colliding protons into a production target to produce pions, which subsequently decay into muons. The muons collide with an aluminum stopping target, where muons will be captured by the aluminum nuclei. If neutrino-less muon to electron decay occurs, an electron with a distinct energy signature of 105 MeV will be observed.

One event that can mimic this signal is radiative pion capture, where a pion is captured by the nucleus of an aluminum atom in the stopping target and emits a high energy photon. This photon can convert into an electron and positron pair near the signal energy. To avoid this, signals that occur before the pion decay are excluded as background. Pions out-of-time with the beam pulse are not so easily excluded, and thus beam extinction rate must be kept extremely low to reduce this background. Two devices are planned to measure this. The Precision Timing Profile Monitor (PTPM) which we will focus on is to be installed downstream of the Delivery ring, and will monitor the extinction rate in the Recycler and the Mu2e beam to the order of 10^{-5}. This monitor will be placed upstream of the 'AC Dipole System,' a system of resonant dipoles and collimators that will provide the final required extinction for the experiment. Downstream of this system, the Target Extinction Monitor will measure the beam down to final required extinction rate of 10^{-10}.

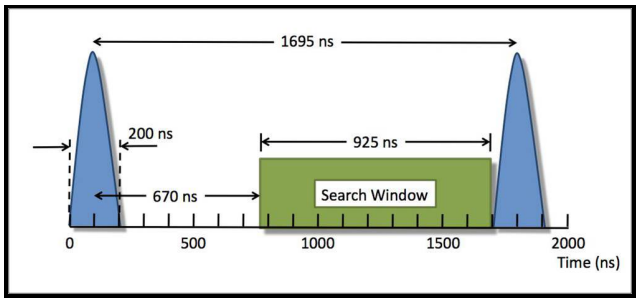

Figure 1: Mu2e will utilize a pulsed proton beam with bunches on the order of a muon lifetime apart. This beam will collide with the production target to produce pions which decay to muons. By limiting the timing of the search window to after all pions have decayed, backgrounds from radiative pion capture can be eliminated. However, out-of-time protons can produce out-of-time pions that still appear in this window.

The PTPM will consist of four arms each with four Quartz Cherenkov Radiators to detect protons scattered off of a thin target in the beam. Detecting a small number of scattered protons, as opposed to placing detectors directly in the beamline, prevents the high intensity of the beam from saturating the sensitive detectors. By integrating over many bunches, we will have a statistical profile of the out-of-time protons which can be used to calculate the extinction rate.

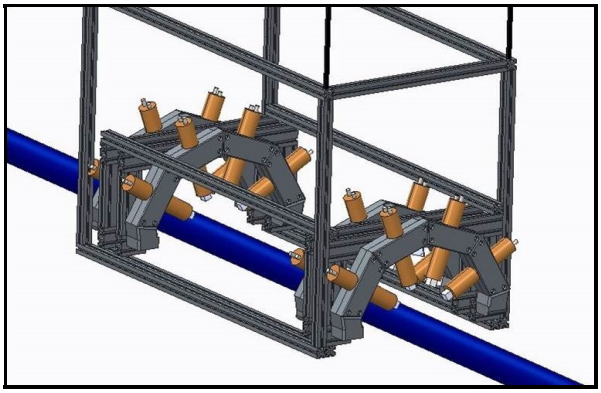

Figure 2: This PTPM will monitor the extinction rate of the proton beam in the Fermilab Recycler and upstream of the AC Dipole System to 10^{-5}. The PTPM will consist of four arms of four Quartz Cherenkov radiators to detect protons scattered off a thin target in the beam. From this we can produce a statistical profile of out-of-time protons.

Quartz Cherenkov Radiators use Cherenkov light to detect particles. When a charged particle, such as a proton, travels through a medium faster than light can travel through the medium, it produces a light shockwave that can be amplified by a photomultiplier tube (PMT). Light produced in this way is called Cherenkov light. For quartz, a particle must have a $\beta \geq .707$ to produce light.

Quartz Cherenkov Radiators were chosen because they are insensitive to soft (low energy) background particles, have a very fast response, and do not have much afterglow after large signals. One tradeoff is that they produce a weaker signal than scintillators of a similar size. The goal of this beam test is to analyze the response of the Quartz to relativistic protons to verify that it will meet our needs.

3 Apparatus:

This experiment was conducted at the Fermilab Test Beam Facility (MTest) using a 120GeV pulsed proton beam with 19ns RF buckets. The data shown in this paper is for low rate beam (about 2000 triggers/spill), although we also tested beam up to about 190,000 triggers/spill. Four 2.54cm x 2.54cm x 2.54 cm Quartz Radiators were attached to Hamamatsu R7056 PMTs and mounted approximately 30cm apart with hose clamps on a one meter piece of extruded aluminum. The aluminum was mounted on a remotely controlled motion table that permitted alignment in the horizontal and vertical planes. Two scintillators with surface areas 2.1cm x 2.2cm x .6cm (upstream) and 1.3cm x 1.5cm x .6cm (downstream) were attached to PMTs and mounted to the walls of the enclosure in line with the test beam.

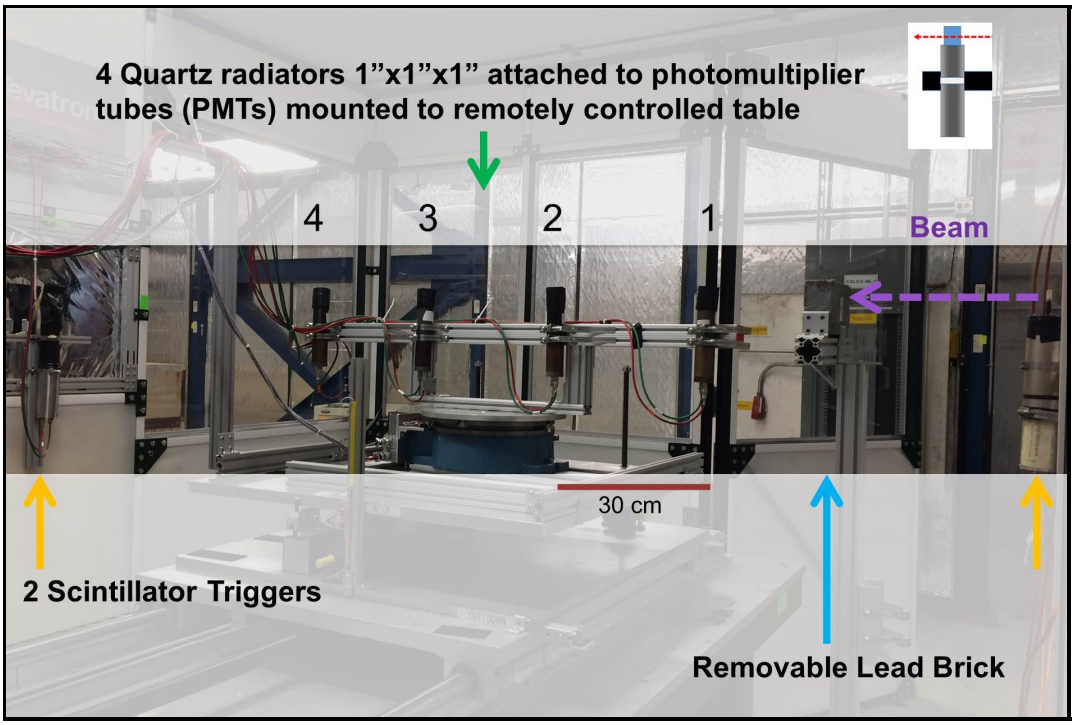

Figure 3: Our beam test was conducted at the Fermilab Test Beam Facility (MTest) using 120GeV protons. Coincidence of two scintillators shown, as well as three scintillators in the test beam hall, were used as a trigger. The data shown in this paper was taken at low intensity (about 2000 triggers/spill), with the lead brick absent unless specified.

Signals were read using a Agilent InfiniiVision MSO7000 Oscilloscope that was triggered on the coincidence of the two described scintillators, plus three scintillators in the test beam hall. Nuclear Instrumentation Modules (NIMs) were used to require coincidence for a trigger to occur. Signals were converted to text files using a C++ program and analyzed using root macros. The arrival time of a signal was defined as the time of the steepest negative derivative of the signal.

Data was also taken using a 5.08cm thick lead brick 40cm upstream of the first quartz to create a hadronic shower on the detectors. We expected the hadronic shower to cause multiple charged particles, such as pions, to pass through the quartz simultaneously, resulting in larger signals. These large signals could be used to look for saturation in our detectors. A g4beamline simulation was used to predict the particle species that should interact with our detectors.

4 Results and Discussion:

Our detector produced measureable signals in all four tracks. An example track is shown in figure 4.

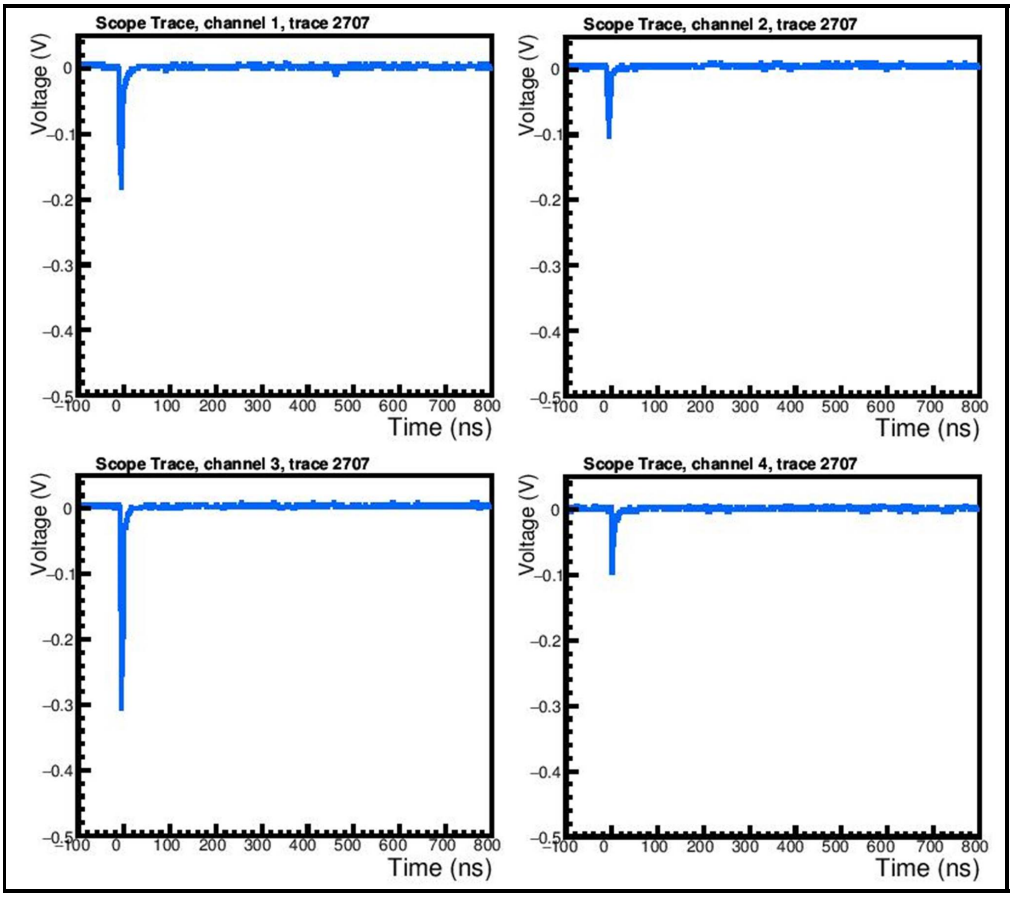

Figure 4: A sample quadruple coincidence event. A single track between -50ns and 10ns occurs and no other signals are found in the timing window examined.

We analyzed the signal amplitude in figure 5. Signals were negative with means of (-.24 ± .08)V, (-.11 ± .05)V, (-.21 ± .08)V, and (-.12 ±.06)V for Quartz 1-4 respectively.

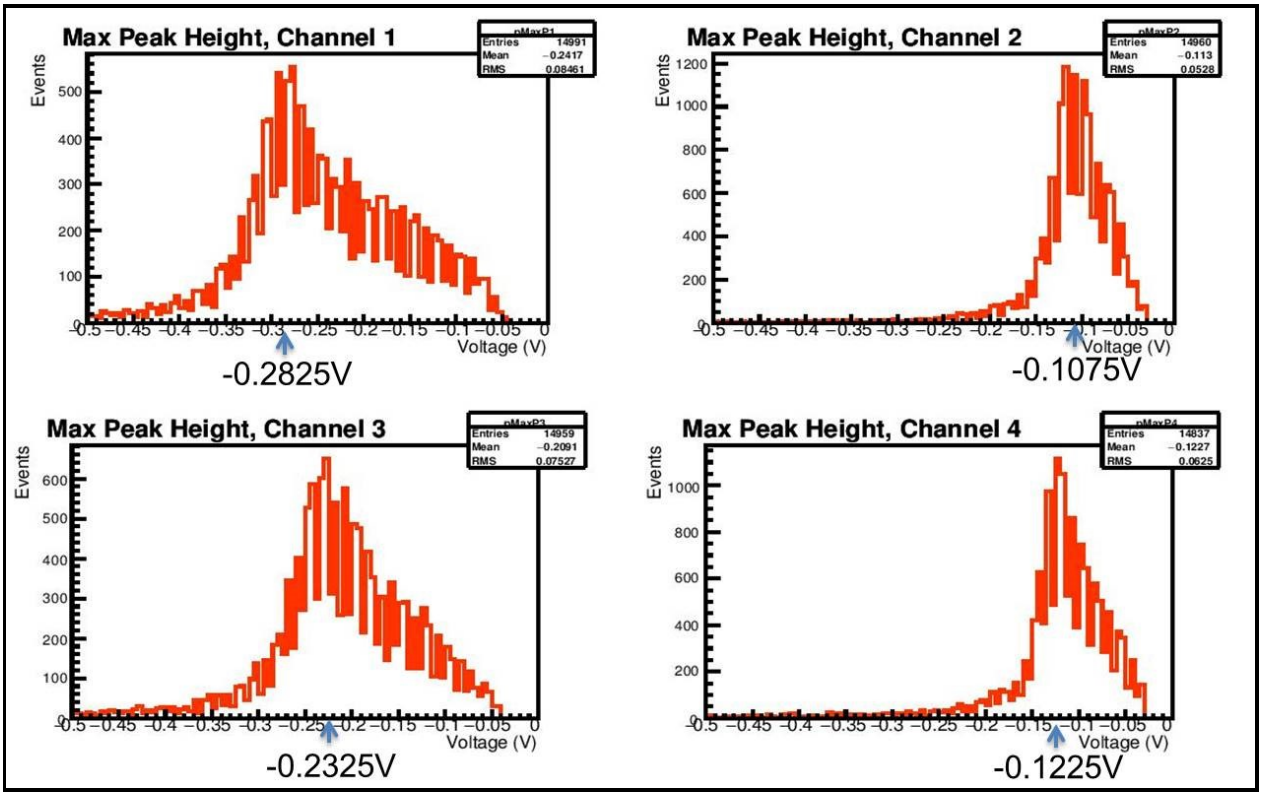

Figure 5: The signal amplitudes for in-time protons follow an approximately Gaussian distribution that is different for each channel. The amplitude of the signal was defined as the maximum signal occurring within the in-time arrival window for each record. The label below the voltage axis describes the maximum of the distribution.

In order to count signals, we must set a threshold for signal height. Signals stronger than the threshold (have an absolute value greater than the threshold) will be counted, while lesser signals will be excluded as noise. To do this, we constructed plots of the number of total peaks versus threshold and of efficiency versus threshold, as shown in figures 6 and 7.

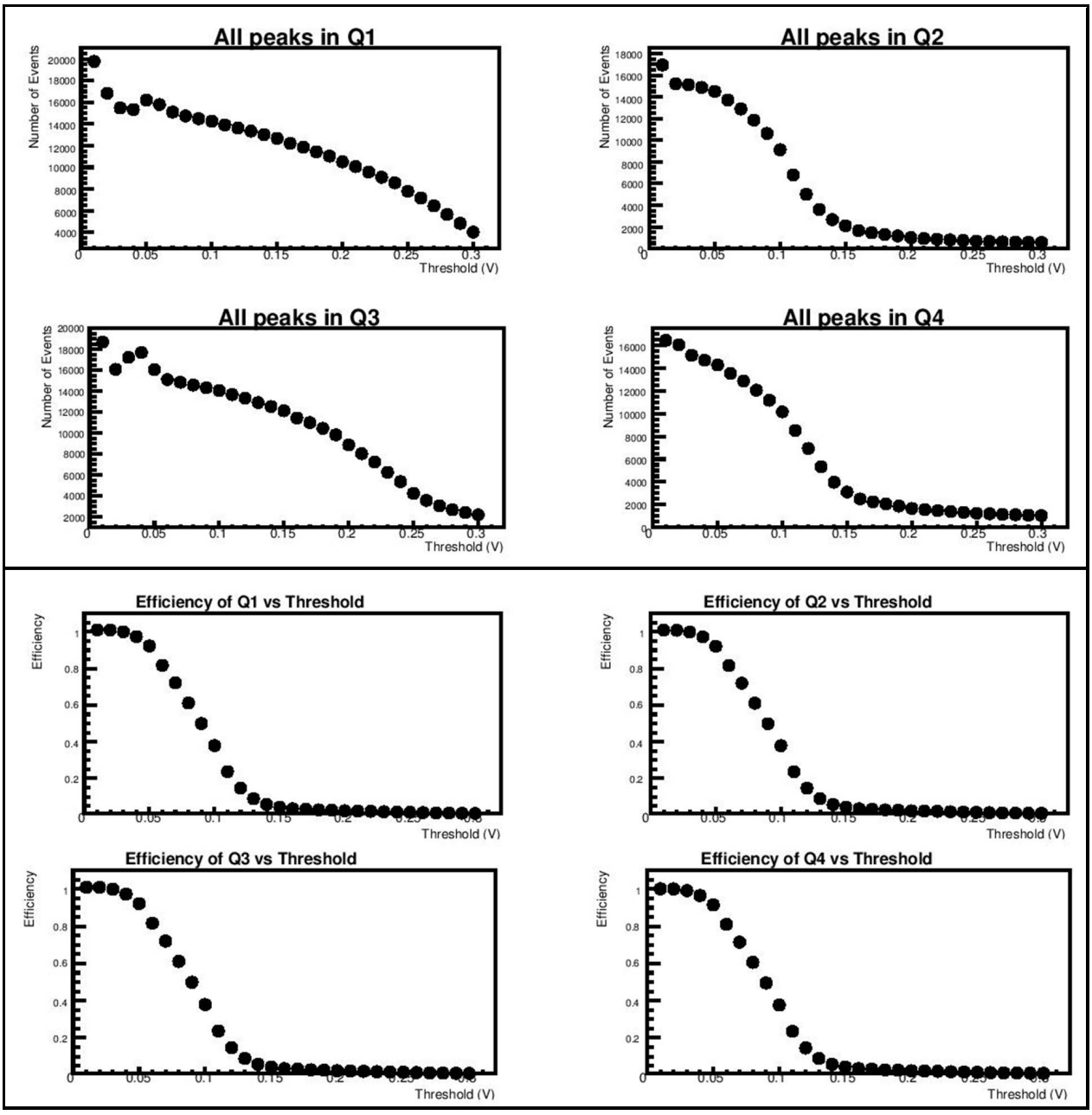

Figure 6: The number of signals ("peaks") above threshold is graphed for thresholds between .01V and .3V, allowing for multiple peaks in each record. The resultant efficiency is also graphed. Efficiency is defined in figure 8. 15000 records are represented here.

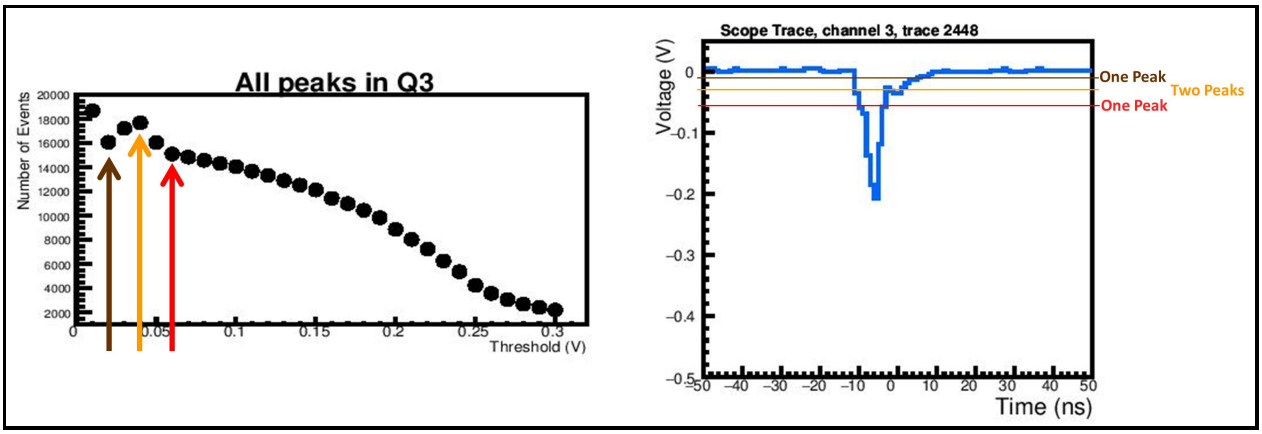

Figure 7: The slight dip seen in the number of signals ("peaks") observed in Quartz 1 and 3 is due to peak structure. Our peak finding algorithm requires for a peak to dip below threshold before it searches for a second peak. Thus, if the peak has structure, an intermediate threshold may observe more peaks than a slightly lower or slightly higher threshold. Ideally, we would like to avoid this intermediate threshold to avoid double counting peaks.

From the plots in figure 6, we balanced the effect of the value with which efficiency fell off steeply with trying to avoid double-counting a peak due to peak structure. We determined the absolute value of the thresholds for Quartz 1-4 to be .04V, .03V, .04V and .03V respectively. Using these thresholds, I then calculated the efficiency for detecting protons passing through the detector, as shown in figure 8.

$$\text{Efficiency}_{\text{Quartz (\#)}} = \frac{\text{Number of Quadruple Coincidences}}{\text{Number of Triple Coincidences in other Three Channels}}$$

$$\text{FourFold Efficiency} = \text{Efficiency}_{Q1} \bullet \text{Efficiency}_{Q2} \bullet \text{Efficiency}_{Q3} \bullet \text{Efficiency}_{Q4}$$

15000 events	Quadruple Coinc.	Triple Coinc.	Efficiency
Quartz 1	14771	14775	(99.97 ± .02)%
Quartz 2	14771	14804	(99.78 ± .02)%
Quartz 3	14771	14792	(99.86 ± .02)%
Quartz 4	14771	14912	(99.05 ± .02)%
Four-Fold Efficiency			(98.67 ± .05)%

Figure 8: Efficiency for a single Quartz is defined as the ratio of quadruple coincidences (records that have an in-time signal in all four Quartz), to triple coincidences (records that have an in-time signal in the three Quartz other than the Quartz of interest). The four-fold efficiency is the product of the efficiencies for each quartz.

As shown in figure 8, we achieve an efficiency of detecting protons of (98.67 ± .05)%, which is very close to unity. I next looked at the arrival time of in-time signals, as shown in figure 8. The trigger occurs at 0ns. In-time signals were defined to be the maximum signal occuring between -50ns to 0ns for Quartz 1-3, and -50ns to 10ns for Quartz 4.

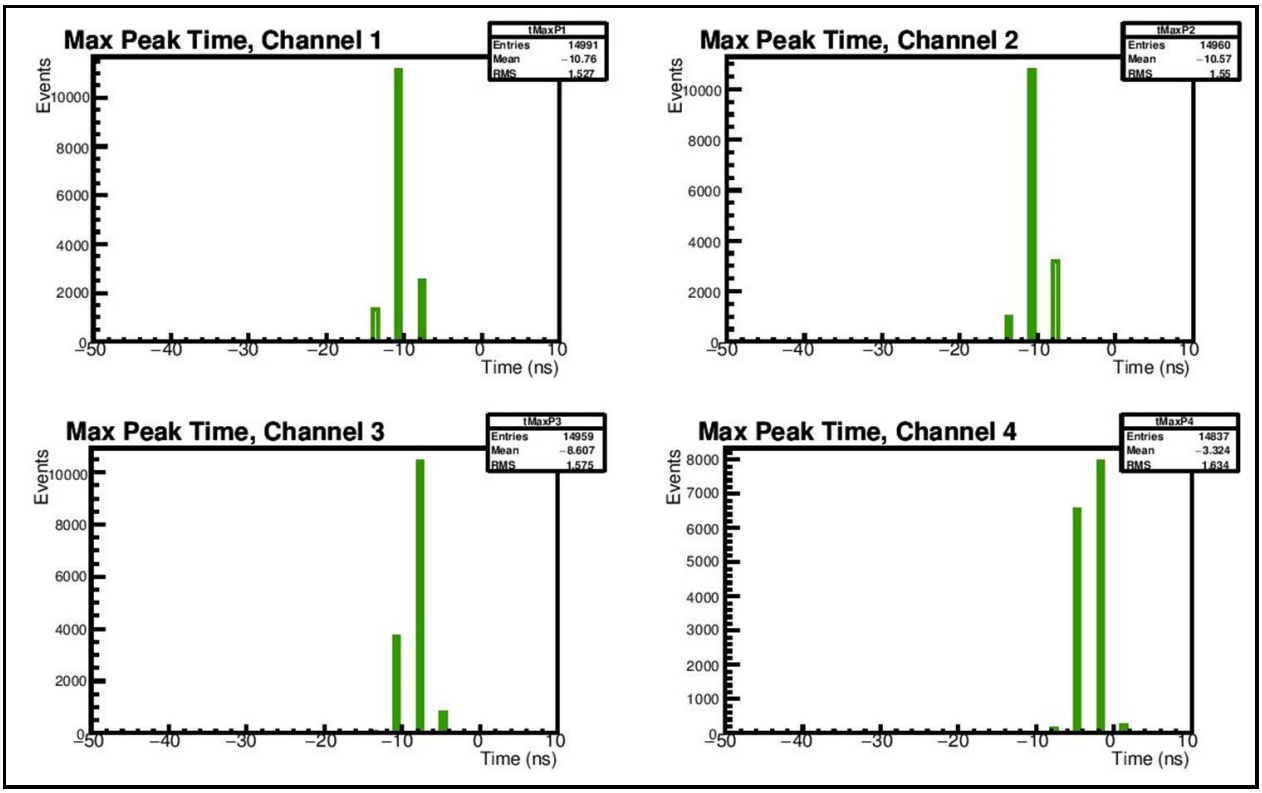

Figure 9: The signal time for protons arriving in our in-time window (-50 ns to 0ns for Quartz 1,2,3 and -50ns to 10ns for Quartz 4). The signals appear to arrive before the trigger (0ns) because the Quartz signals passed through less wire and electronics to arrive at the oscilloscope.

Using the difference between these plots, I calculated the timing resolution as shown in figure 9.

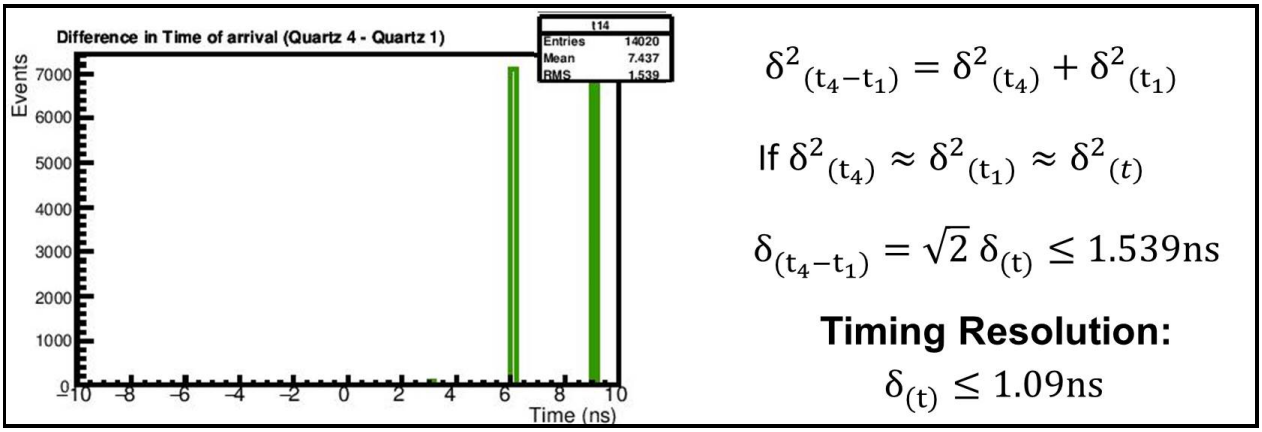

Figure 10: The timing resolution was calculated for a single channel using the RMS of the difference in arrival times between two channels. The difference between channels 1 and 4 had the largest RMS (1.539ns), and thus it was used as the limit for our timing resolution.

We achieved a timing resolution of 1.09ns for the arrival time of our signal. This is smaller than the RMS of any individual quartz, whose RMSs are given in figure 9 as 1.527ns, 1.55ns,

1.575ns, and 1.634ns for Quartz 1-4 respectively.

I then analyzed out-of-time signals, which were defined to be 40ns to 800ns after the trigger. The timing of the out-of-time signals was nearly random, although in 26000 records there were 41 out-of-time signals in Quartz 1 and 71 out-of-time signals in Quartz 3 occurring around 100ns after the trigger. This may be after pulsing occurring at a low rate. To estimate the probability of this time structure producing false quadruple coincidences, I tested how often an out-of-time signal would have a coincidence (signal within 20ns) with the previous record in the same quartz. The rate of quadruple coincidence is then the product of this self-coincidence for all four quartz. This described self-coincidence never occured in our data set, so afterpulsing has at worst a 2 x 10^{-18} probability of producing a false quadruple coincidence.

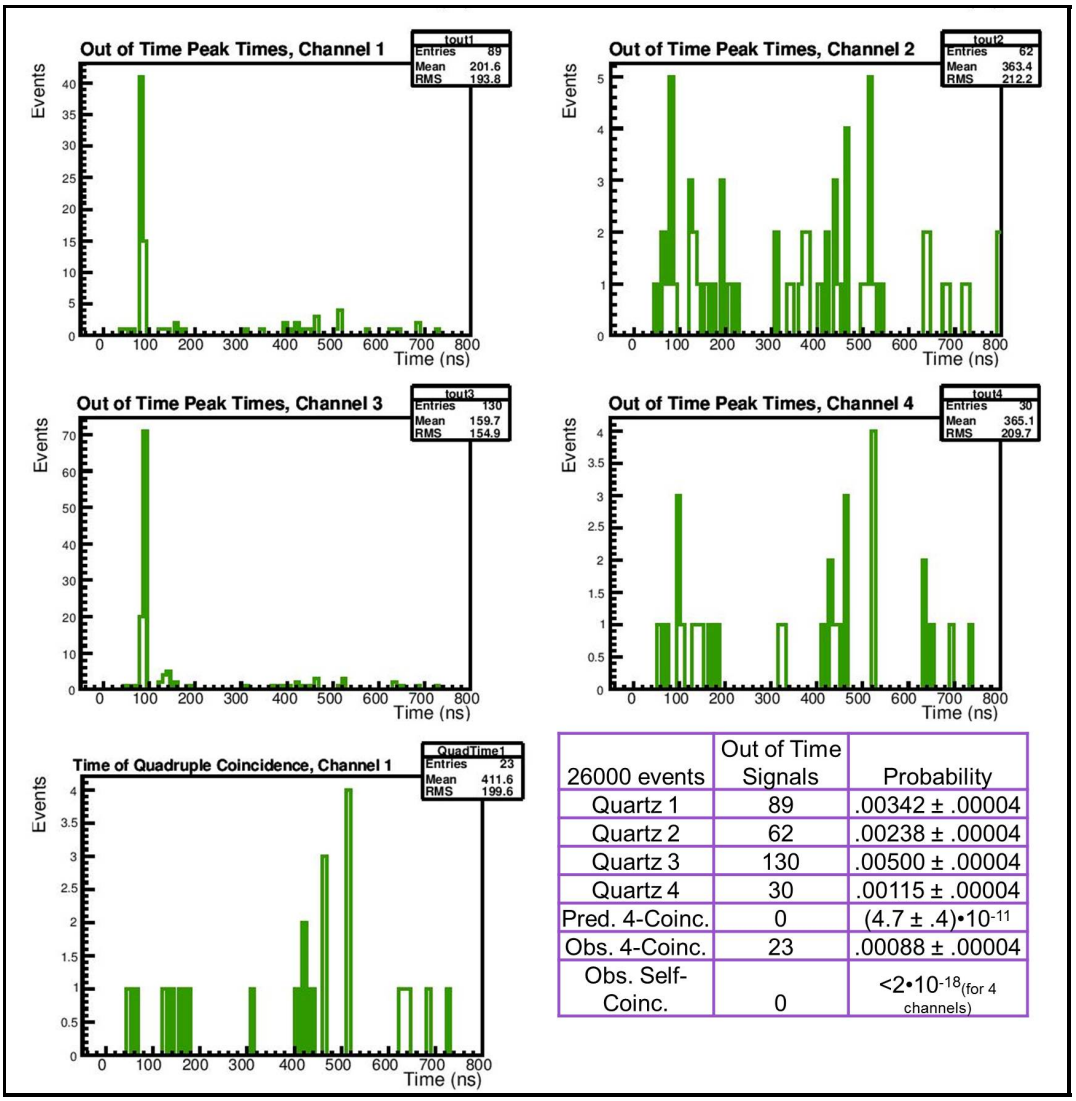

26000 events	Out of Time Signals	Probability
Quartz 1	89	.00342 ± .00004
Quartz 2	62	.00238 ± .00004
Quartz 3	130	.00500 ± .00004
Quartz 4	30	.00115 ± .00004
Pred. 4-Coinc.	0	$(4.7 \pm .4) \cdot 10^{-11}$
Obs. 4-Coinc.	23	.00088 ± .00004
Obs. Self-Coinc.	0	$<2 \cdot 10^{-18}$ (for 4 channels)

Figure 11: Time distribution and counts for out-of-time signals (40ns to 800ns) for 26000 events. Quadruple coincidences were required to be within 20ns of each other. Arrival time is nearly random, especially for 4-coincidences. There may be after pulsing occurring at a low rate around 100ns for Quartz 1 and 3. I tested how often a record with an out-of-time signal had an out-of-time signal in the previous record of the same channel. This never occurred in our data set, and thus this effect has at worst a 2 x 10^{-18} probability of producing a false 4-coincidence.

The observed quadruple coincidence rate, .00088 ±.00004, was much greater than the quadruple coincidence rate that would be predicted by random coincidence of the single out-of-time events (4.7 ±.4)x 10^{-11}. This suggests that the quadruple coincidences we observed were caused by actual out-of-time protons instead of after pulsing, electronic effects or cosmic rays. Looking at individual tracks, signals that are part of a quadruple coincidence resemble signals produced by in-time protons. Out-of-time signals that are not part of a quadruple coincidence are usually smaller, and have a different look as shown in figure 12.

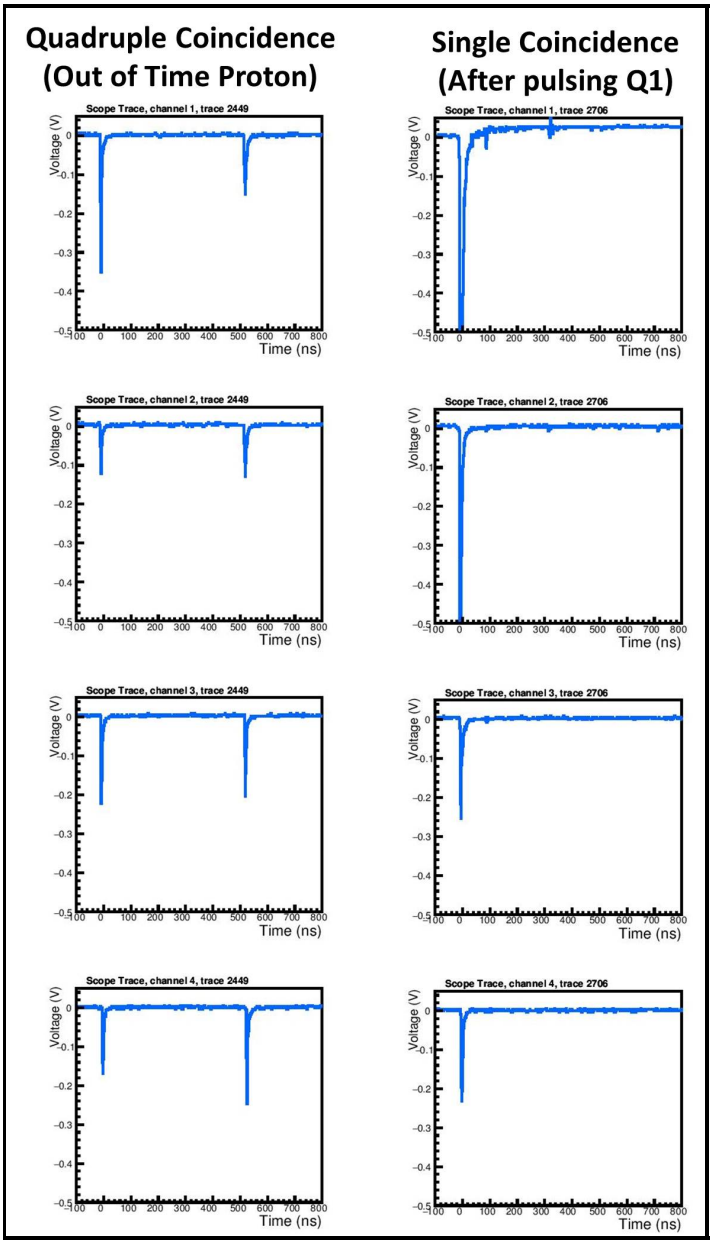

Figure 12: Two events displaying an in-time signal and an out-of-time signal. Out-of-time signals, such as shown in the event on the left, typically produce signals in all four tracks and are from out-of-time protons. Out-of-time backgrounds, such as shown in Quartz 1 in the event on the right, may come from electronic noise, cosmic rays, or after pulsing, and are more likely to appear only in one track.

Near the end of our beam test we installed a lead brick about 40cm upstream of the first Quartz Radiator to create a hadronic shower on our detectors. We expected the primary content of the hadronic shower to be pions, as shown on the left side of figure 13. Pions are somewhat massive, and thus more likely to stay close to the center of the beam after production and pass through multiple quartz. Thus, occasionally we should see tracks where two pions passed through the detector simultaneously, leaving large tracks in all channels. However, we did not see as strong of correlation between the signal heights in each channel as we would expect. Thus we went back and ran some simulations to better educate our expectations of what particles are passing through our quartz.

I ran a simulation using g4beamline of a 120GeV proton beam striking a lead brick installed 40cm upstream of 4 quartz cubes 30cm apart. The simulation predicted the species and momentum of particles passing through our cubes. Figure 14 shows the total number of protons, electrons and positively charged pions with a $\beta \geq .75$ (slightly larger than the required .707 to ensure the signals are large) that are predicted to pass through each quartz radiator if 20000 protons arrive at the lead brick. Most of the protons pass through the lead brick and continue on to hit the quartz. Others interact and produce particles such as electrons and pions. We were surprised to see that electrons (and positrons) are generally more prevalent than charged pions.

Electrons are produced as shown on the right side of figure 14, from neutral pions that decay to gamma photons. These photons then produce electron positron pairs. Electrons and positrons are much lighter than pions, and are less likely to follow the beam trajectory after production. Thus, it is less likely that an electron and a positron pass through the quartz simultaneously, and thus large signals from multiple charged particles passing through the quartz simultaneously are less likely, especially in the downstream quartz.

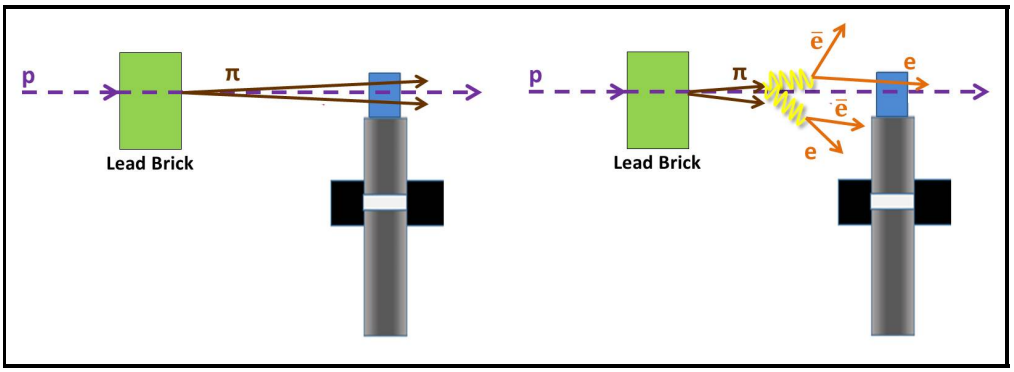

Figure 13: Two possible hadronic shower products that may pass through our quartz radiators. If pions are produced, their comparatively larger mass keeps them closer to the center of the beam, and thus it is likely that multiple pions will pass through the detector simultaneously. However, neutral pions will decay into gamma photons which then produce electron positron pairs. Electrons and positrons have comparatively smaller masses and thus are less likely to hit the detector simultaneously.

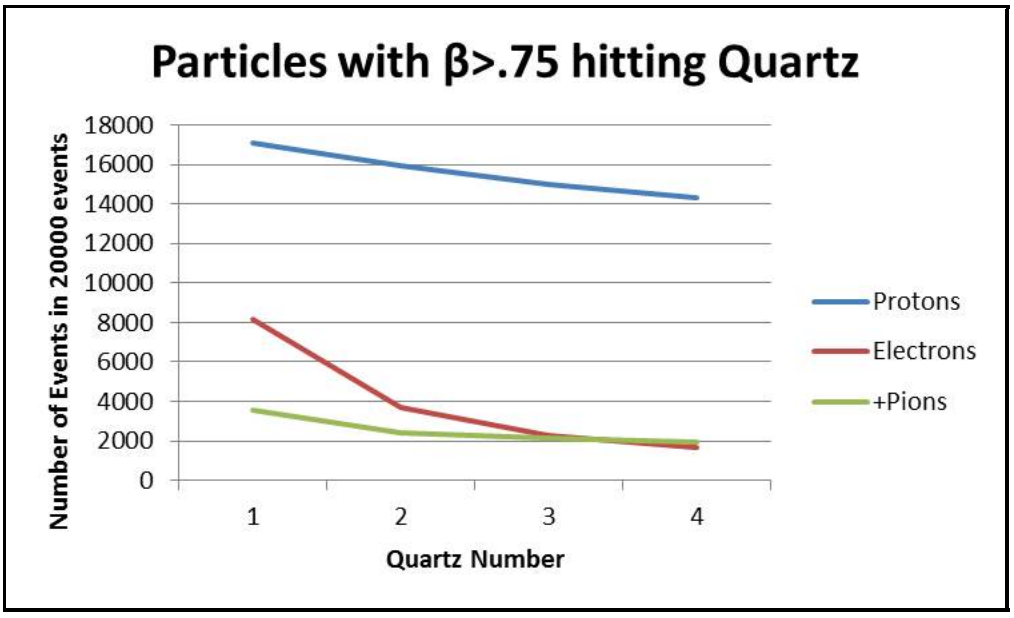

Figure 14: Our g4beamline simulation predicted the number of protons, electrons, and positively charged pions that should interact with our quartz if 20000 protons arrive at the lead brick.

In the context of this electron dominated shower, we can begin to make sense of the lack of correlation in signal height. Figure 15 shows a comparison of normalized signal height for each event measured between multiple quartz. There is some correlation between Quartz 1 and Quartz 2, but only spotty correlation between any of the other quartz. Similar plots generated from data without the lead brick (not shown) display even less correlation between signal heights, which would be expected as beam protons arrive individually. Only when multiple particles arrive in the detector simultaneously should the signal heights have a strong correlation. Our simulation shows that our products are dominated by protons and electrons, which we generally do not expect to produce correlation between the signal heights. Electrons and positrons are more likely to be close together in the upstream part of the detector, and thus the greatest correlation occurs between Quartz 1 and 2. The pions in the beam do produce some correlation between the remaining quartz, but this is largely drowned out by the proton and electron signals.

I can to a certain extent reproduce these plots using our simulation. Instead of plotting signal heights (which are dependent on the response of the detectors to the particles) we plotted the number of particles passing through the detector for a given proton that interacted with the lead brick. If multiple particles pass through the detector simultaneously, this is analogous to a larger signal in the quartz. This representation is shown in figure 16. This also shows the trend that the strongest correlation occurs between Quartz 1 and 2, with lesser correlations occurring between the other quartz. In general, the correlation is still better in the simulation than in the experiment, but due to imperfections and the Gaussian spread of the beam this is to be expected.

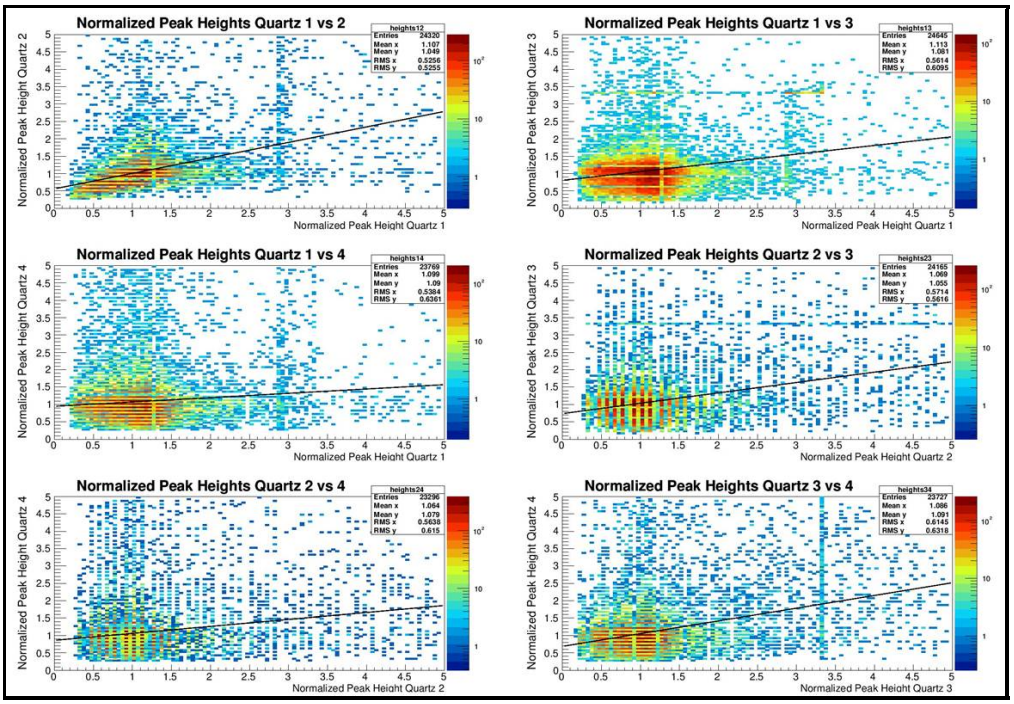

Figure 15: The normalized signal height was compared between Quartz Radiators. The normalized signal height was defined as the maximum in-time signal height divided by the mean signal height for the respective quartz. The greatest correlation occurs between Quartz 1 and 2.

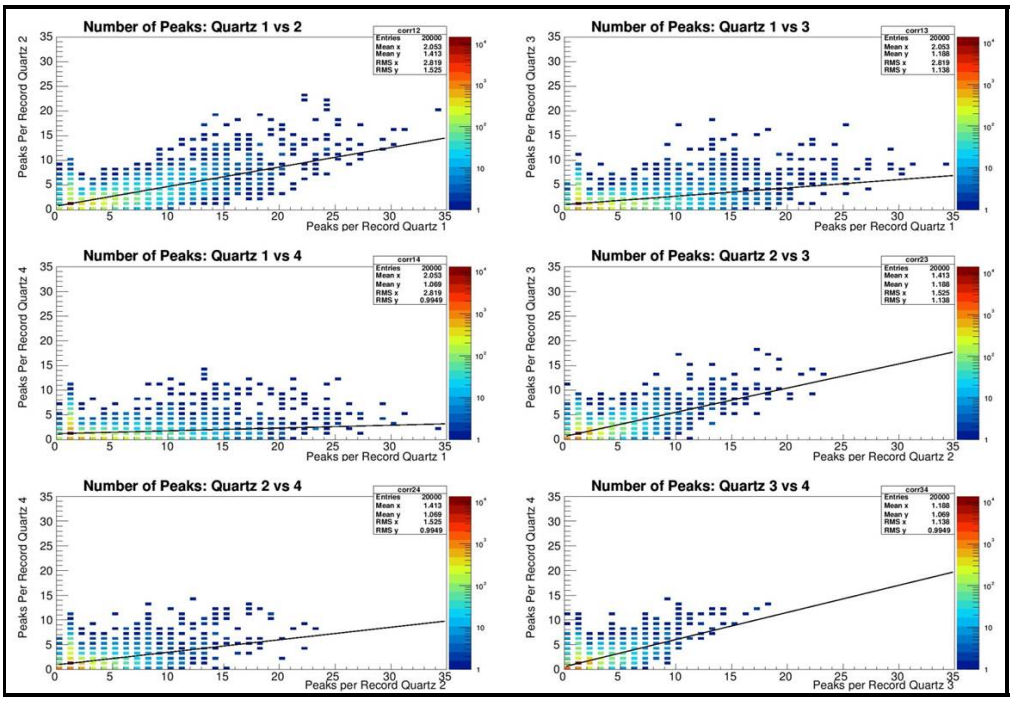

Figure 16: The number of particles passing through each quartz for a given proton arriving at the lead brick is compared between Quartz Radiators. The particles were required to have a $\beta \geq .75$. The greatest correlation occurs between Quartz 1 and 2.

Although explainable, this lack of correlation and predominance of electron events in our hadronic shower limits the usefulness of our lead brick test in observing saturation in the detectors. Further analysis of the data should be able to find dual pion events and look for saturation, however these events will be much rarer than we initially anticipated.

Another interesting note about the lead brick data is that it showed slightly more time structure in the arrival of out-of-time peaks. The self-coincidence test as performed on the non-lead brick data in figure 11 was also performed on the lead brick data. The number of self-coincidences observed in 25000 events was, for 6, 2, 0, and 1 for Quartz 1-4 respectively. This means the rate of quadruple coincidence due to after pulsing is at worst 1 x 10^{-16}, two orders of magnitude larger than the limit placed for the data taken without the lead brick. Certain after pulsing events, such as the one displayed on the right side of figure 12, show after pulsing associated with a large signal that may cause saturation in the quartz. Although we would need further analysis to confirm, perhaps this increased rate of after pulsing is associated with an increased rate of saturation in the quartz.

5 Summary and Future Directions:

Our results show strong indications that Quartz Cherenkov Radiators will meet the needs of this PTPM. The four quartz radiators tested achieved an efficiency of (98.67 ± .05)% for detecting protons with time resolution of 1.09ns. The signals produced by the quartz radiators were measureable and distinct, with mean amplitudes of (-.24 ± .08)V, (-.11 ± .05)V, (-.21 ± .08)V, and (-.12 ± .06)V for Quartz 1-4 respectively. After pulsing is estimated to only produce quadruple coincidences at a rate of 2 x 10^{-18}, many orders of magnitude below the 10^{-5} order at which this PTPM will measure.

Further analysis of the data taken with the lead brick in place can help us better understand saturation in our detectors, and whether this phenomena is involved in after pulsing. The increased time structure in after pulsing observed in our lead brick data may be associated with an increased rate of saturation in our detectors, but further analysis would be required to confirm this.

References

[1] C. B. Mott, Research and Development for the Mu2e Extinction Monitor, M.S. Thesis, Physics Dept., Northern Illinois Univ., De Kalb, IL, 2016.

[2] E. Prebys, M. Jamison-Koenig, L. Rudd, Tests of Quartz Radiators for Beam Precision Timing Monitor. Beams-doc #5018-v3, 2015.

[3] L. Rudd, Characterization of Quartz Radiators for Mu2e Upstream Extinction Monitor, Beams-doc #5016-v1, 2015.

[4] D. Hedin, E. Prebys, Technical Scope of Work for the 2016 Fermilab Test Beam Facility Program, Beams-doc #5203-v1.

[5] Muons Inc., G4beamline Beam Tracking Simulation Software, Version 3.02.1. http://www.muonsinternal.com/muons3/G4beamline